



Thermal oxidative degradation of an epoxy resin

Nathalie Rose, Michel Le Bras, René Delobel

Laboratoire de Physicochimie des Solides, ENSCL, Université des Sciences et Technologies de Lille, BP 108, F-59652 Villeneuve d'Ascq Cedex, France

&

Bruno Costes & Yves Henry

Aérospatiale 12, Rue Pasteur F-92152 Suresnes, France

(Received 2 March 1993; accepted 29 March 1993)

This study of the thermodegradation of the tetraglycidyl diamino diphenyl methane/diaminodiphenylsulfone system (TGDDM/DDS) defines the different steps of the carbonization process. It characterizes, in particular, the domain of existence of an expanded carbonaceous structure which is constituted of small domains of turbostratic carbon. Moreover, this present work discusses the role of oxygen in the formation of this structure and shows that there is competition between the carbonization process and the oxidative degradation.

INTRODUCTION

Epoxy resins are widely used in the aeronautic industry. They constitute the organic matrix for high performances composite materials with reinforcement fibers, used for fabrication of light structural panels in the interior of aircraft. The analysis of several accidents¹ has shown the total implication of these materials in fire propagation and flash-over phenomena (total flare-up of gases). In all the cases, the concentration of gases and smoke generated involves, if not the death, a partial or total incapacity of occupants limiting their possibility to survive by a rapid evacuation.² Then, there is a considerable reinforcement of different regulations (FFA) and these new safety requirements seriously limit the number of materials used in habitable areas. It is necessary to improve the fire resistance of these materials and this requires a better understanding of their degradation.

Among the different epoxy resins, the tetraglycidyl diamino diphenyl methane/diamino-

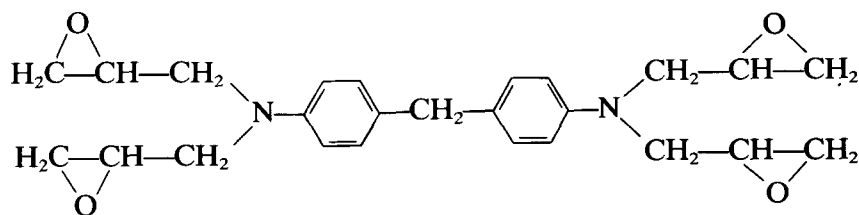
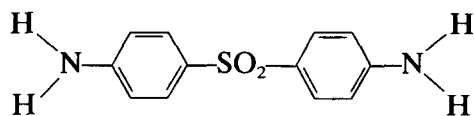
diphenylsulfone (TGDDM/DDS) system has been largely used. Its chemical properties and polymerization reactions are well known.³

The present work deals with the thermodegradation process of this epoxy resin TGDDM/DDS (*N*-glycidyle/aromatic amine). The thermal stability was studied by thermogravimetric (TG) analysis under air and inert gas (N_2) flow. The spectroscopic characterizations were carried out by IR, Raman, XRD, EPR, and ^{13}C solid-state NMR.

EXPERIMENTAL

Materials

The tetra epoxy prepolymer TGDDM is a commercial product (Lopox B3302) characterized by a functionality of 3.6 (theoretical 4). The formulation studied in this work contains 52.5 parts of curing agent per hundred parts of resin (phr) which corresponds to a stoichiometric ratio TGDDM/DDS with one epoxy group for each primary amino hydrogen on the DDS.

TGDDM (*N,N,N',N'* tetraglycidyl-4,4'diamino diphenyl methane)

DDS (diamino 4,4' diphenylsulfone)

The TGDDM/DDS mixture was prepared by continuously stirring the curing agent into the resin heated at 100°C until a clear mixture was obtained. The homogeneous mixture was then out gassed at 100°C for 20 min, cooled to room temperature and stored at -20°C in a freezer until use.

Thermoset epoxy resins are processed by cure, i.e. conversion of liquid monomers into a three-dimensional thermoset network via chemical reactions.³ The first reaction is the attack of a primary amine on an epoxy group on a side chain. This may be followed by two types of cross-linking reactions, intermolecular and intramolecular.

The resin was cured with the following procedure: 1 h at 135°C and a postcure at 180°C for 2 h. The epoxy consumed was around 90%.³

The spectroscopic characterizations were restricted to samples resulting from isothermal treatments (6 h under air) at temperatures deduced from TG analysis and noted HTT (higher treatment temperature).

Thermal analysis

Thermogravimetric analyses were carried out with temperature programming (heating rate: 3°C/min) under synthetic air (Air Liquid grade) or under inert gas (N₂, Air Liquid U grade) flows (5 × 10⁻⁷ m³/s) using a Setaram MTB 10-8 microbalance. In each case, the mass was fixed at 20 × 10⁻⁶ kg and the samples were positioned in open vitreous silica pans. The precision on the temperature measurement was ±1.5°C in the range 50-650°C.

Spectroscopic analysis

Raman microprobe examination was performed with a Raman microspectrometer having spectrographic dispersion and multichannel detection (Microdil 28- Dilor). An optical beam produced by a continuous wave argon laser enters in a microscope and is directed on to an objective that focuses it to a one-micrometer spot on the sample surface. To avoid sample heating the power was kept below 4 mW. Subsequent visual examination of the surface was systematically made in order to check that no alteration had occurred around the focal point. In a typical experiment, the laser beam wavelength was fixed at 514.5 nm and the value of spectral slit width at 9 cm⁻¹.

¹³C NMR measurements were performed on a Bruker CXP 100 weak field spectrometer at 25.2 MHz (2.35 T) with magic-angle spinning (MAS), high power ¹H decoupling and ¹H-¹³C cross-polarization (CP). The Hartmann-Hahn matching condition was obtained by adjusting the power on the ¹H channel for a maximum ¹³C FID signal of adamantane. All spectra were acquired with a single contact time of 5 ms. A repetition time of 10 s was used for all samples because the spin-lattice relaxation time (*T*₁) always stayed below 2 s at all temperatures (the repetition delay is chosen five times *T*₁). Typically 10 000 scans were necessary to obtain spectra with a good signal/noise ratio and the reference used was tetramethylsilane (TMS). All spectra of the solids were obtained at the spinning speed of 3 kHz.

EPR spectra were recorded at 25°C using a Varian 'E line' spectrophotometer. A frequency of 9.5 × 10⁹ Hz (X band), a Klystron modulation of 100 kHz, and a Varian 'strong pitch' standard were used. The scan was recorded on a scale of 40 G during 480 s with a time constant of 0.1 s and a peak-to-peak modulation amplitude fixed at 0.5 G. Saturation measurements were made by determining the peak-to-peak amplitude *D* of the

first derivative EPR curve as a function of microwave power (BPP plot).⁴ The ratio $R_S = (D/P^{1/2})/(D_u/P_u^{1/2})$ is equal to 1 in the absence of saturation. In this relation, P is the variable micropower, and P_u and D_u are respectively one power level in the unsaturated regime and the corresponding peak-to-peak amplitude. The concentration of the paramagnetic species was computed by using a method of integration of the signal previously described by Raymond.⁵

IR spectra were recorded in the range 4000–300 cm^{-1} using a Perkin–Elmer 683 instrument connected with a PE 3600 data station. The samples were obtained by powdering in KBr in adequate ratio to obtain transmission values above 15%.

RX patterns were recorded on a Siemens D500 diffractometer with powder patterns (40 KeV, 20 mA, $K\alpha_{1,2}$ of Cu,Ni monochromator).

RESULTS

The thermal stability of the cured epoxy resin TGDDM/DDS was evaluated by thermogravimetric analysis under air. The TG curve and the first derivative curve (DTG) are shown in Fig. 1. The thermal degradation starts from

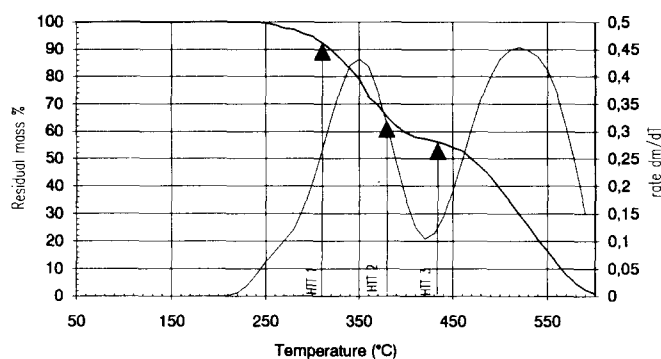


Fig. 1. TG and DTG curves in air of TGDDM/DDS 1/1 cured (arrows indicate the three characteristic temperatures discussed in text).

250°C and the rates of weight loss are maximal at 350 and 520°C. The last step leads to a complete degradation of the material.

To follow the evolution process, the authors have chosen some characteristic temperatures where it is interesting to study the residue formed after an isothermal treatment (6 h).

- 310°C permits study of an intermediate product characterizing the first step;
- 380°C is characteristic of the second step; and
- 430°C represents the last step. This was chosen in order to recover enough solid residue; the residual mass after an isothermal treatment at 430°C, during 6 h, is low: 6% (Table 1).

Some characteristics of these residues are summarized in the Table 1. In particular, it is interesting to note that, for 380°C, there is formation of soot and a swelling and foaming of the material which corresponds to the formation of an intumescent structure.

The residues were first characterized by elemental analysis. Figure 2 presents the changes of the ratios of weight percentages H/C, N/C, O/C and S/C.

After a heat treatment at 310°C, the ratio O/C decreased strongly compared with its initial value. It may be assumed that a dehydration reaction proposed by numerous authors^{6,7} occurs with elimination of two alcohol functions to form an ether bond.

At higher temperatures, above 310°C, S/C and H/C decrease, which may be explained respectively by an evolution of SO_2 and a dehydrogenation process. This last phenomenon may correspond either to a dealkylation of hydrocarbon structures involving the formation of volatiles or to the development of a condensation process which would lead to the formation of polyaromatic structures.

From 310°C, we can also observe an enhancement of the N/C ratio. It may be

Table 1. Description of isothermally heat treated samples

HTT (°C)	Residual mass after isothermal treatment (%)	Soot	Aspect of residue	Swelling and foaming of the material surface
310	74.7	No	Tough and bright; brown powder	No
380	22	Yes	Crumbly; black powder	Yes
430	6.3	Yes	Crumbly; black powder	Yes

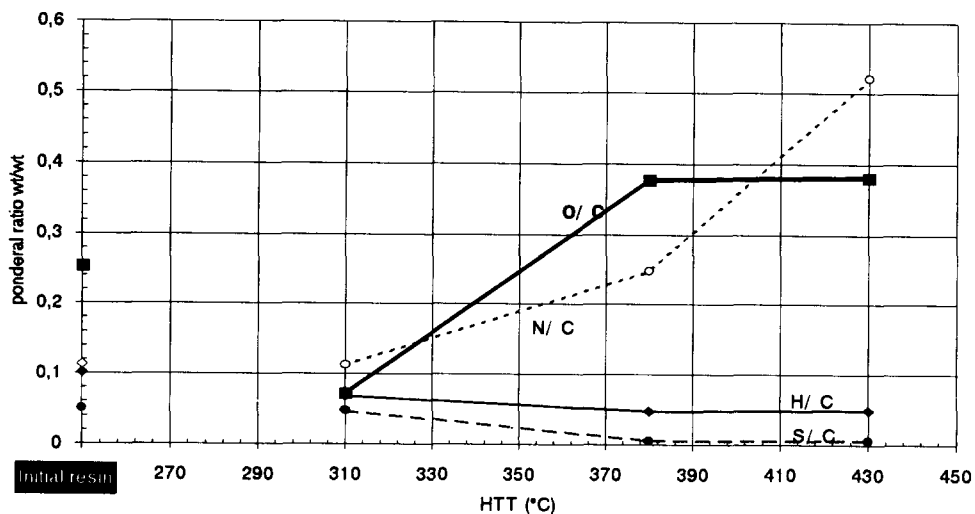


Fig. 2. H/C, O/C, N/C and S/C ratios versus HTT.

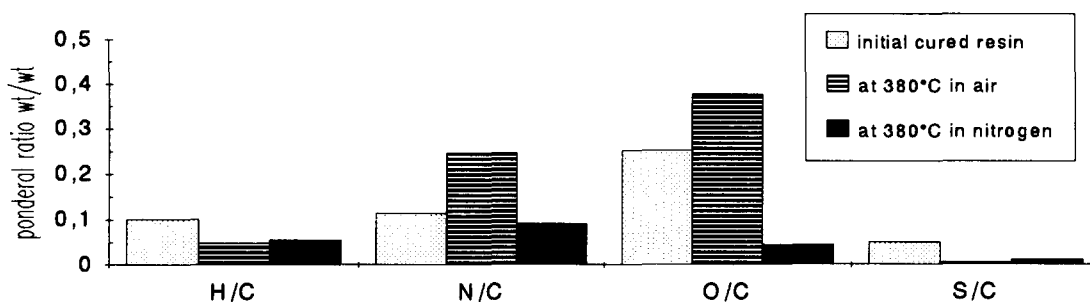


Fig. 3. Elemental analysis of solid residue obtained at 380°C in air and in N₂.

considered that the nitrogen may be implicated in heat resistant cyclized structures more stable than the carbonaceous structures.

The increase of the O/C ratio, above 310°C, may be related to an oxidation process of the polymer chains by molecular oxygen. This result is confirmed by treatment at 380°C in nitrogen

atmosphere which leads to a decrease of the ratio O/C (Fig. 3).

For a better understanding of the oxidation phenomenon, we can compare the TG curve of the cured resin obtained under an inert gas (N₂) flow and in air (Fig. 4). The amount of residue between 250 and 520°C is higher in thermo-

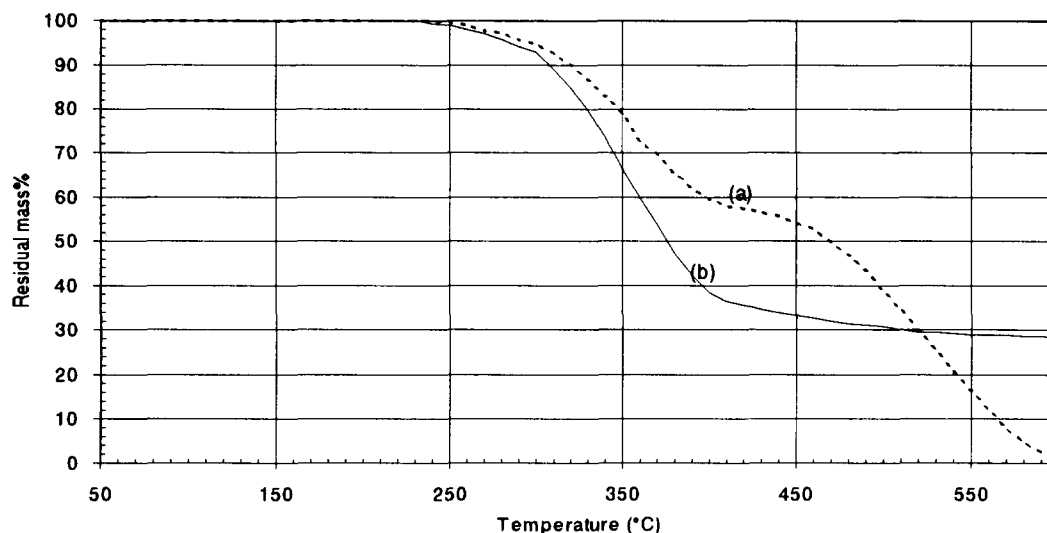


Fig. 4. TG curves of TGDDM/DDS 1/1 in air (a) and in N₂(b).

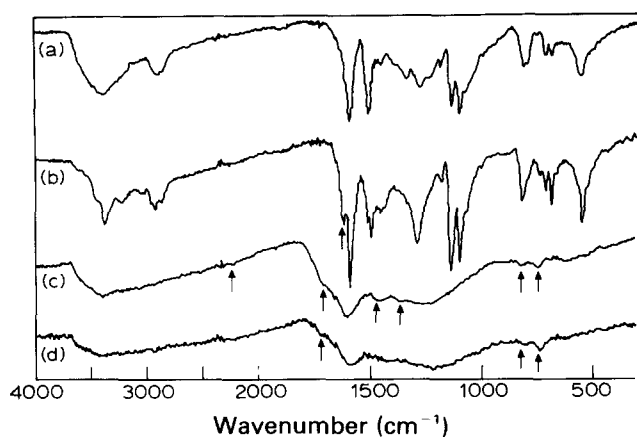


Fig. 5. IR spectra of TGDDM/DDS 1/1 cured (a) and after thermal treatment at 310°C (b), 380°C (c) and 430°C (d).

oxidative conditions than under inert gas. However, at higher temperatures, in air a complete degradation of material occurs, whereas in nitrogen atmosphere the amount of residue remains constant (about 30%).

Thus, it seems that the oxygen permits retention of good thermal properties during the degradation process, but up to 460°C the rate of weight loss increases and the degradation becomes complete.

In order to understand the degradation process, spectroscopic studies have been carried out with samples treated at temperatures previously defined.

Figure 5 compares IR spectra obtained after thermal treatment. The spectrum of the residue obtained at 310°C is unchanged compared with the initial sample, for which the assignments have been previously proposed by Costes.³ However, between 310 and 380°C significant change is observed and spectra at 380 and 430°C show large absorptions which make the assignments difficult.

Nevertheless, the presence of hydrocarbonaceous species is characterized by absorption bands at 1370 and 1470 cm^{-1} assigned respectively to the deformation mode, symmetric and antisymmetric, of alkyl groups bonded to aromatic cycles.^{8,9} Moreover, the presence of polyaromatic species is proved by the absorptions at 830 and 759 cm^{-1} assigned to the deformation mode of the aromatic CH.¹⁰⁻¹² The presence of a band at 1720 cm^{-1} may be assigned to C=O species, and the band at 2240 cm^{-1} indicates the presence of CO₂ adsorbed. Thus, from 380°C there is formation of oxidized products probably formed by a reaction with molecular oxygen.

In conclusion, IR spectroscopy permits us to

observe from 380°C both oxidation and the formation of polyaromatic species in the residue.

Raman microspectroscopy has been used to specify the nature of polyaromatic species. The Raman spectrum of a sample treated at 380°C (Fig. 6) exhibits two broad bands around 1580 and 1350 cm^{-1} , which are generally assigned to carbon or carbon precursors. The diffuse band at 1580 cm^{-1} corresponds to the E_{2g} vibrational mode (C—C vibration in the aromatic layers). The band at 1350 cm^{-1} is assigned to A_{1g} vibrational mode and may be related to the structural organization of the carbonaceous material.^{13,14}

Lespade *et al.* have studied the Raman spectra of a tar pitch versus their graphitization ratios and proposed the reactional scheme described in Fig. 7.^{15,16} We can conclude, in the authors' case, that the residue obtained at 380°C corresponds either to phase I, or to phase II, or to a mixture of these two phases.

These results confirm the beginning of development of a structured carbonaceous material at this temperature.

X-ray diffraction allows us to specify the nature and the size of the carbonaceous structure and to evaluate its structural state. Figure 8 represents diffraction spectra of samples treated respectively at 310, 380 and 430°C. The initial resin shows a broad band at 0–9° that implies a low order in the network. This order is preserved after a treatment at 310°C. For samples treated at 380 and 430°C, a new broad band appears at around 12° which is assigned to (002) scatterings of turbostratic carbons.^{17,18} This structure is made up of polyaromatic species which grow by arranging in parallel layers.^{19,20}

Interlayer spacings and crystal sizes of turbostratic carbons are obtained respectively by application of the Bragg and Scherrer equations to the experimental X-ray scattering profile.^{20,21} The results are in Table 2.

The interlayer spacing *d* decreases slightly with temperature which implies a beginning of structural ordering. Moreover, the development of crystal size remains low.

In conclusion, the X-ray diffraction study indicates the formation of small domains of turbostratic carbon in the high temperature residues (*T* > 310°C). This expanded carbonaceous structure is very interesting. Indeed, it could limit the transfer to heat in the material.

To obtain more information about the

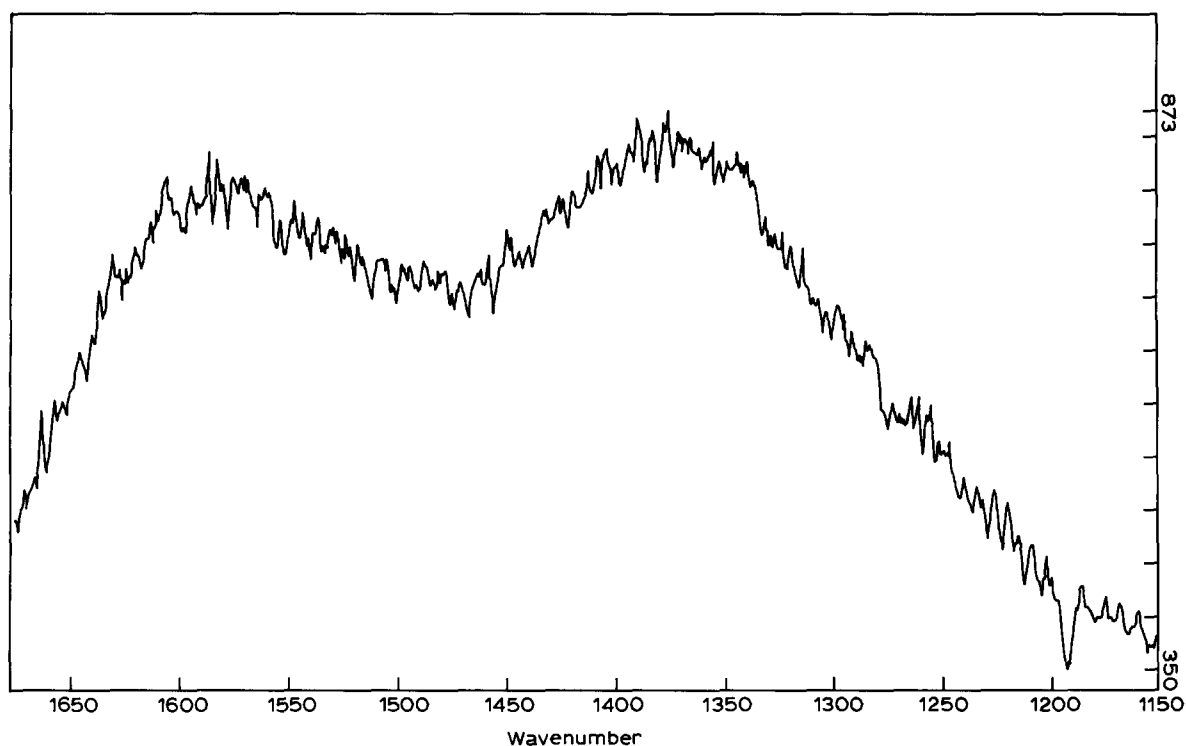


Fig. 6. Raman spectrum of resin treated at 380°C in air.

formation of these carbonaceous structures, an electron paramagnetic resonance (EPR) spectroscopic study on the samples has been carried out.

The resonance spectra are characterized by: the spectroscopic splitting factor g , the resonance line shape factor $K = B/A$ (estimated using the slope method²²) and the free radical concentration n (Fig. 9).

Figures 10–12 present the changes in these parameters with the higher treatment temperature (HTT). The presence of paramagnetic

species may be assigned, according to Singer *et al.*,⁴ to trapped free radicals, which may result from a charring process of the material.

The value of the splitting factor g for residues obtained is around 2.004 (Fig. 11), which corresponds to the value for a pitch, so this agrees with the hypothesis of such material. Figure 12 shows that the free radical concentration increases until 380°C (about 10^{18} spins g^{-1}).

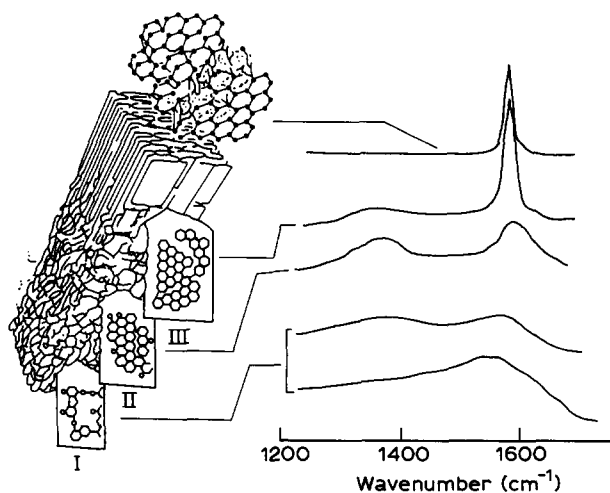


Fig. 7. Change of the Raman spectrum of a tar pitch with graphitization ratio.¹⁵

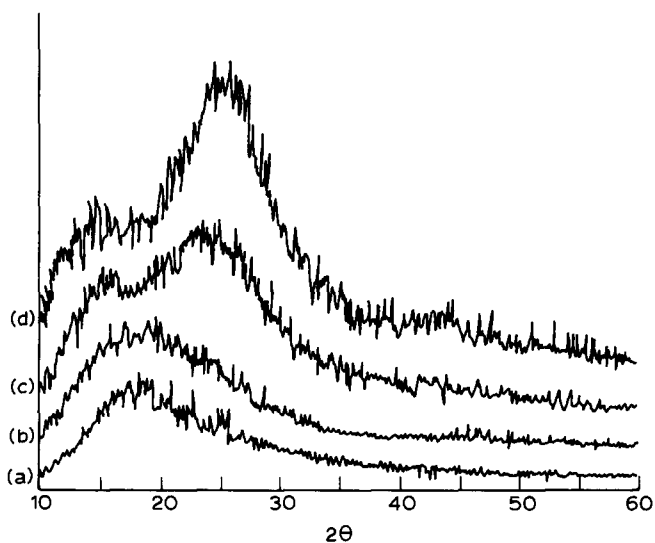


Fig. 8. X-ray diffraction profiles of TGDDM/DDS 1/1 cured (a) and after thermal treatment at 310°C (b), 380°C (c) and 430°C (d).

Table 2. Characteristics of the X-ray diffraction profiles of TGDDM/DDS 1/1 as function of the high temperature of treatment (HTT)

HTT (°C)	Bragg angles θ (°)	Interlayer spacings d_{002} (Å)	Full at half maximum $\beta_{1/2}$ (in 2θ radians)	Crystal size t (nm)
Initial cured resin	9	4.9	—	—
310	9	4.9	—	—
380	12	3.7	8	1.26
430	13	3.4	6	1.67

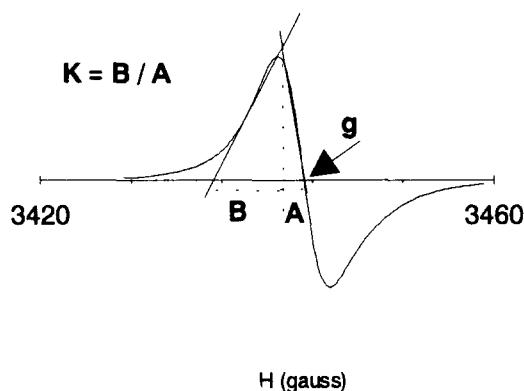


Fig. 9. Schematic of EPR spectra.

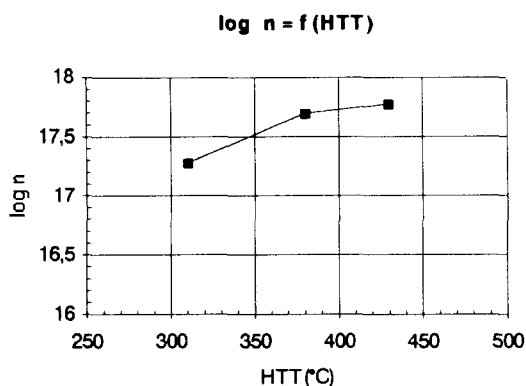


Fig. 12. Variation of the paramagnetic species concentrations versus HTT.

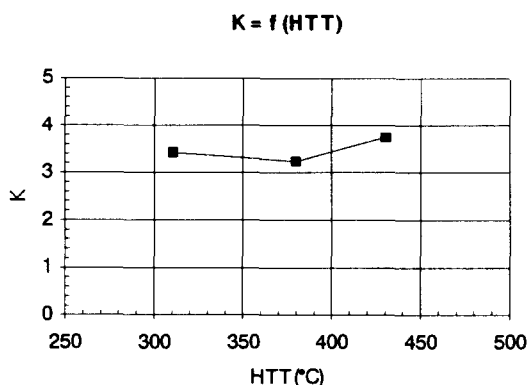


Fig. 10. Variation of the resonance line shape factor K versus HTT.

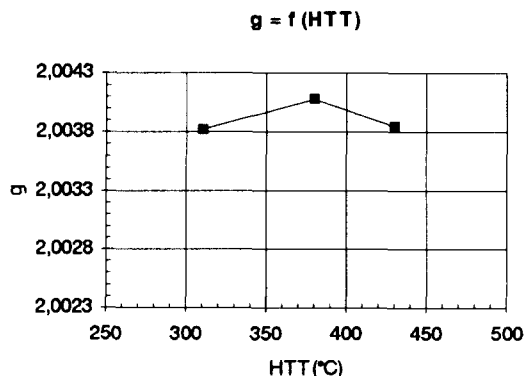


Fig. 11. Variation of the spectroscopic splitting factor g versus HTT.

These radicals may be created by the formation of polyaromatic structures or may be associated to the formation of oxidized species. Between 380 and 430°C the concentration of free radicals remains relatively constant, which may imply a competition between the development of a condensation process of polyaromatic species and chain breaking.

Line shapes give information about the types of interactions between a spin system and its environment (Fig. 13).⁴ In a simple homogeneous system, the relaxation process is controlled by spin–lattice interactions and the energy absorbed from the radiation field is distributed so that the spin system maintains thermal equilibrium throughout the resonance process. In this case, theory predicts that the line shape should be Lorentzian. On the other hand, in an inhomogeneous spin system, the individual electrons find themselves in different local fields so that resonance does not occur for all the spins simultaneously. The individual relaxations of all these spin systems add up to form a Gaussian signal. For distinguishing Lorentzian or Gaussian shapes, the slope method illustrated in Fig. 9 was used. The ratio of slopes B/A is 4 for a Lorentzian curve and 2 for a Gaussian one (Fig. 13).⁴

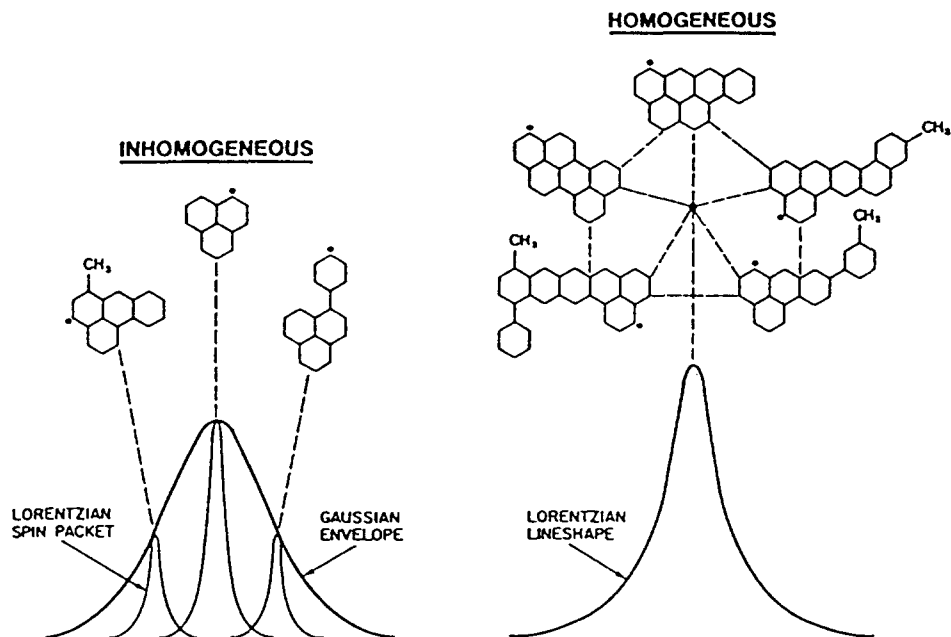


Fig. 13. Depiction of the relationship between molecular structure, molecular interactions, EPR line shapes, and spin relaxation mechanisms.⁴

The observed signals for each heat treated samples are Lorentzian lines characterized by a value of K around 4 (Fig. 10).

This result indicates a mechanism of homogeneous relaxation, so that the spins have identical interactions. It may be proposed that the mechanism of carbonization involves only one main radical species, probably a polyaromatic macromolecule which has trapped a free radical.

This technique allows us to confirm the condensation of polyaromatic structures above 310°C by a carbonization free radical process.

A study by ^{13}C solid-state NMR nuclear magnetic resonance spectroscopy CP/MAS (cross polarization/magic-angle spinning) has been carried out to characterize the chemical groups of the carbonaceous species obtained during the degradation. Figure 14 shows the spectra of the cured resin TGDDM/DDS obtained at the different temperatures. Two ranges are defined: the first between 100 and 150 ppm (characteristic of aromatic carbons) and the other between 30 and 80 ppm (characteristic of mobile side chains of the backbone). The values and the assignments of chemical shifts are listed in Table 3.

The interpretation of the spectra of the initial cured resin (Fig. 14(a)) was made from the literature.^{1,23,24} The band at 150 ppm is characteristic of aromatic carbons in amines. The bands at 130 and 114 ppm are respectively assigned to the C3, C4 and C2 aromatic carbons drawn in

formula at the top of the figure. The assignments of the large band between 30 and 80 ppm was made by Grenier-Loustalot and Grenier in comparison with the chemical shifts of model compounds^{23,24} (Table 3).

When the sample is heat treated at 310°C, the corresponding NMR spectrum changes (Fig. 14(b)). Indeed, a broadening of the band, characteristic of the aromatic carbons, between 150 and 100 ppm is observed. Its maximum is noted at 130 ppm. Moreover, new lines are observed at 20 and 14 ppm which may be assigned to alkyl groups bonded to aromatic rings. This result shows that there is a destruction of the initial network and some breakdown reactions.

For the residues obtained at 380 and 430°C, the spectra present no characteristic bands of aliphatic carbons. The broadness of the 128 ppm line reflects the condensation of the polyaromatic structures. Moreover, a new band at 156 ppm shows the presence of oxygenated aromatic structures, which become more important at 430°C compared with the polyaromatic structures.

In conclusion, this method confirms the degradation mode of the resins. From 310°C, there are scission reactions along the macromolecule chain which lead to the formation of polyaromatic structures and, concurrently, an oxidation process which leads to the formation of

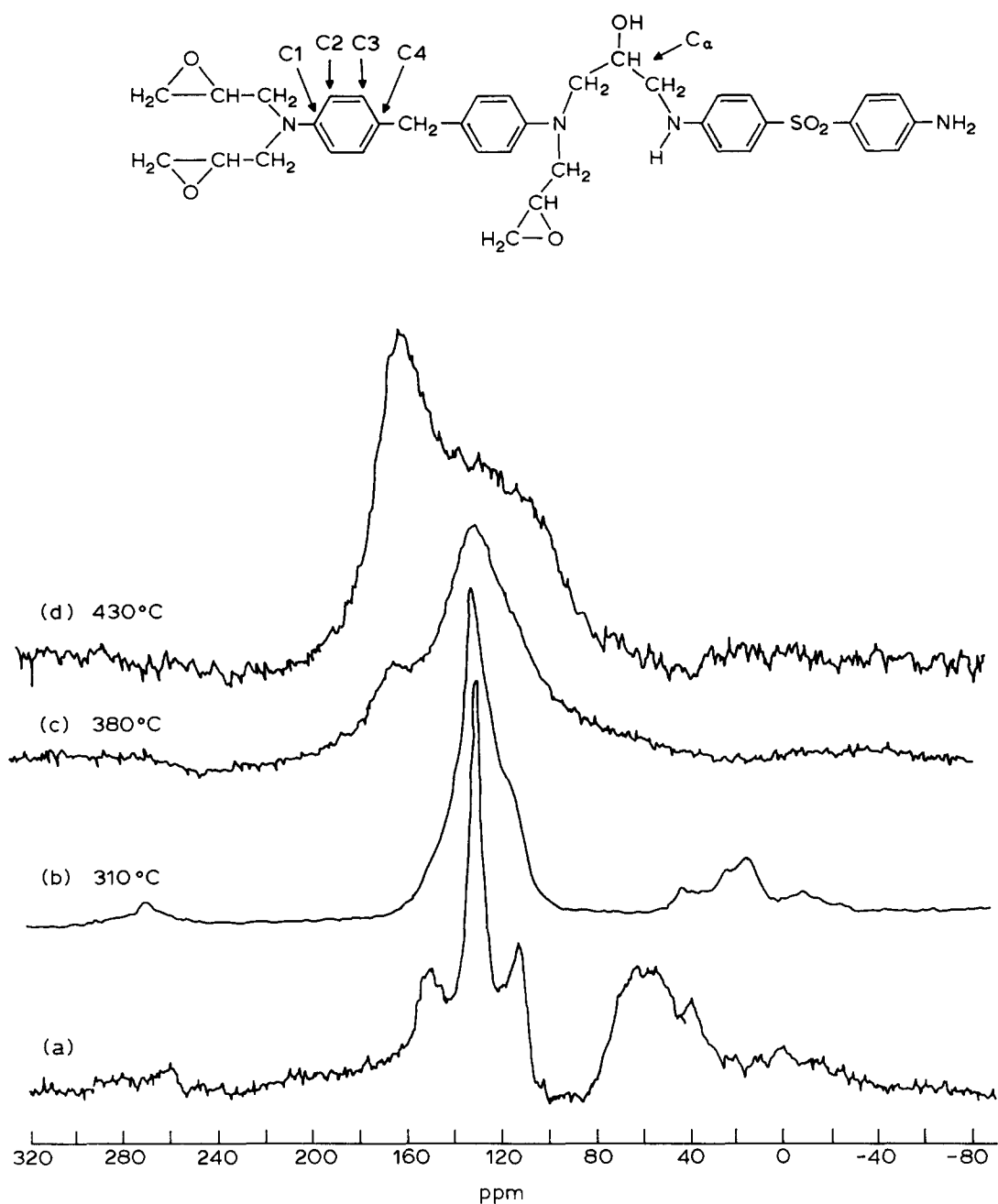


Fig. 14. Characteristics of the ^{13}C MAS.N.M.R. spectra of TGDDM/DDS 1/1 cured (a) and after thermal treatment at 310°C (b), 380°C (c) and 430°C (d).

oxygenated aromatic structures. These last structures are favored when the temperature increases. We can conclude that there is a competition between the carbonization process and the oxidative degradation.

CONCLUSION

Thermal analysis of an epoxy resin TGDDM/DDS shows that, at low treatment

temperatures ($T < 310^\circ\text{C}$), the mechanism of degradation is identical in air or under inert atmosphere; it corresponds principally to a dehydration reaction.

At higher temperatures ($T > 310^\circ\text{C}$), an evolution of SO_2 can be suspected which is a problem in view of toxicology and environmental safety.

Spectroscopic characterization of the residue shows that there is formation of small domains of turbostratic carbon above 310°C. This structure is

Table 3. Assignments of the chemical shifts of ^{13}C CP/MAS NMR spectra of the initial epoxy resin and the residue obtained at 310, 380 and 430°C

HTT (°C)	Chemical shifts (ppm)	Assignments	Refs
Initial cured resin	150	Aromatic carbon C ₁ —N	1, 23, 24
	130	Aromatic carbons C ₃ and C ₄	1, 23, 24
TGDDM/DDS 1/1	114	Aromatic carbon C ₂	1, 23, 24
	Large band {	Methylene between aromatic rings	23, 24
		Alcohol	23, 24
		Ether bonds	23, 24
310°C	129	Aromatic carbons C ₃ and C ₄	25
	112 (shoulder)	Aromatic carbon C ₂	25
	40	Methylene between the aromatic rings	23, 24
	20	Methyl on aromatic rings	26
	14	Alkyl groups	26
380°C	156	Aromatic oxygenated carbon	25
	122	Aromatic carbons C ₃ and C ₄ and/or polyaromatic	25
430°C	157.7	Aromatic oxygenated carbon	25
	Broad shoulder between 140 and 110	Polyaromatic carbon	25

made up of polyaromatic species lightly organized in parallel layers. There is a beginning of structural ordering.

The results in thermo-oxidative atmosphere show that the oxygen takes part in the degradation and leads to the formation of a material with good thermal properties until 460°C.

REFERENCES

- Costes, B., Bodu, J. J. & Henry, Y., *Charges Minérales et Organiques fonctionnelles dans les Polymère*. Moffis, Le Mans, France (1992).
- Kourtides, D. A., Parker, J. A. & Gilwee, W. J., *J. Fire & Flammability*, **6** (1975) 373.
- Costes, B., Etude structurale du réticulat tetraglycidyl diaminodiphenylmethane (TGMDA) diaminodiphenyl-sulfone (DDS). Thèse, Le Mans, 1989.
- Singer, L. S., Lewis, I. C. & Riffle, D. M., *J. Phys. Chem.*, **91** (1987) 2408–2415.
- Raymond, S. A., *Electron Paramagnetic Resonance*. Wiley-Interscience, New York, 1974, p. 353.
- Morgan, R. J. & Mones, E. T., *J. Appl. Polym. Sci.*, **33** (1987) 999.
- Grayson, M. A. & Wolf, C. J., *J. Polym. Sci., Polym. Phys. Ed.*, **22** (8) (1984) 1897.
- Ouassou, N., Etude d'un nouveau système intumescent 'retard au feu' pyrophosphate diammonique-pentaérythritol. Application au polypropylène. Thèse, Lille, 1991.
- Camino, G., Martinasso, G., Costa, L. & Gobetto, R., *Poly. Deg. & Stab.*, **28** (1990) 24.
- Low, M. J. D. & Morterra, C., *Structure and Reactivity of Surface*, ed. C. Morterra, A. Zecchina & G. Costa. Elsevier Science Publishers, Amsterdam, 1989, p. 607.
- Morterra, G. & Low, M. D., *Carbon*, **21** (3) (1983) 286.
- Wolf, E. E. & Alfani, F., *Catal. Rev. Sci. Eng.*, **24** (3) (1982) 339.
- Lespade, P., Sisse, A. L. & Dresselhaus, M. S., *Carbon*, **20** (5) (1982).
- Nakamizo, N., *Carbon*, **29**(6) (1988) 339.
- Cottinet, D., Couderc, P., Saint Romain, J. L. & Dhamelinourt, P., *Carbon*, **26**(3) (1988) 339–44.
- Lespade, P., Marchal, A., Couzi, M. & Cruege, F., *Carbon*, **22**(4/5) (1984) 375.
- Singer, L.S. Lewis, I. C. & Greinke, R. A., *Mol. Cryst. Liq. Cryst.*, **132** (1986) 65.
- Tse-Haoko & Ping-Chein Chen, *J. Mater. Sci. Lett.*, **10** (1991) 301.
- Lausevic, Z. & Marinkovic, S., *Carbon*, **24**(5) (1986) 575.
- Short, M. A. & Walker, P. L., *Carbon*, **1** (1963) 3.
- Lemaitre, J. L., Goving-Menon, P. & Delannay, F., *Heterogeneous catalyst, Vol. 15*, ed. F. Delannay.. Marcel Dekker, New York, 1984, p. 229.
- Lewis, I. C. & Singer, S., *Chemistry and Physics of Carbon*, 17 ed. P. L. Wather & P. P. Thrower. Marcel Dekker, New York, 1984, pp. 1–88.
- Grenier-Loustalot, M. F. & Grenier, P., *British Polym. J.*, **22** (1990) 303.
- Grenier-Loustalot, M. F. & Grenier, P., *Polymer*, **33**(6) (1992).
- Duncan, T. M. & Douglass, D. C., *Chem. Phys.*, **87** (1984) 339.